# Effect of Al addition on the microstructure and electronic structure of $HfO_2$ film

X. F. Wang and Quan Li[a)]
*Department of Physics, The Chinese University of Hong Kong, Shatin, New Territory, Hong Kong*

R. F. Egerton
*Department of Physics, University of Alberta, Edmonton TG 2J1, Canada*

P. F. Lee and J. Y. Dai
*Department of Applied Physics and Materials Research Center, The Hong Kong Polytechnic University, Hung Hom, Kowloon, Hong Kong*

Z. F. Hou and X. G. Gong
*Department of Physics, Fudan University, Shanghai 200000, China*

(Received 2 June 2006; accepted 27 October 2006; published online 10 January 2007)

We have investigated the microstructures and electronic structures of a series of hafnium aluminate (HfAlO) films with Al concentration ranging from 0% to 100%. When the films evolve from pure $HfO_2$ to pure $Al_2O_3$ by increasing the aluminum content, we find changes in their radial distribution functions, which disclose the short-range order of the materials, despite the amorphous nature of all films. The HfAlO films (with Al/Hf ratio ranging from 0.25 to 5.8) appear to be a single glassy phase of Hf, Al, and O, instead of simple mixtures of $HfO_2$ and $Al_2O_3$. The Hf (Al)–O, Hf (Al)–Al, and Hf–Hf bonds are observed to be insensitive to the amount of Al in the film, except when the Al concentration is large (Al/Hf ~ 5.8), in which case the bonding is similar to that in pure $Al_2O_3$. Although the local symmetry of Hf in amorphous $HfO_2$ is suggested by the electron energy-loss spectrum taken at an oxygen *K* edge, it is largely disrupted when Al is introduced. The valence electron energy-loss spectroscopy reveals three distinct evolving features as the Al content increases, which we discuss in terms of the electronic structure of $HfO_2$. © *2007 American Institute of Physics*. [DOI: 10.1063/1.2405741]

## I. INTRODUCTION

Scaling requirements predict the end of $SiO_2$ as the gate dielectric in complementary metal-oxide-semiconductor (CMOS) integrated-circuit technology, arousing great interest in possible replacements for $SiO_2$.[1–3] Hf-based materials appear to be among the most promising candidates due to their large dielectric constant ($\kappa$), which ensures satisfactory device performance at much larger dielectric thickness compared to that of $SiO_2$, thus solving the problem of large leakage current originating from electron tunneling. Compared to pure $HfO_2$, the addition of Al is found to increase the Si/dielectric interfacial stability[4,5] and the crystallization temperature of the material.[6,7] It is also expected that Al addition will enlarge the band gap of $HfO_2$.[8] Although numerous papers have appeared in the past two years addressing the physical/electrical properties of hafnium aluminate as a gate dielectric,[9–12] the basic microstructure and electronic structure of these amorphous materials remain unclear.

We have carried out a systematic study of the structural evolution of a series of hafnium aluminate films, grown by pulsed laser deposition, as a function of the Al concentration. The short-range order and atomic coordinates of the amorphous hafnium aluminate films are deduced from both the radial distribution functions (RDFs) extracted from the transmission electron diffraction (TED) patterns and the energy-loss near-edge structures of the oxygen *K* edge. The electronic structures of the films are examined by the valence-electron energy-loss spectroscopy (EELS). We discuss the evolution of the microstructure and electronic structure of the films as a function of their Al concentration.

## II. EXPERIMENT

Hafnium aluminate films with thickness of about 20 nm were deposited by pulsed laser deposition onto *p*-type (100) Si substrates, using high-purity hafnium aluminate targets with different Al/Hf ratio (Table I). The silicon substrates were treated with a HF etch just before film deposition, a process that is known to leave the silicon surface terminated by hydrogen. The compositions of the films were examined using x-ray photoelectron spectroscopy (XPS) (PHI Quantum 2000), and their microstructures were investigated by transmission electron microscopy (TEM) (Tecnai 20ST

TABLE I. Al/Hf ratio in the targets and the films.

| Film No. | Al/Hf ratio in the targets | Al/Hf ratio in the films |
|---|---|---|
| HfAlO1 | 0/1 | 0/1 |
| HfAlO2 | 0.5 | 0.25 |
| HfAlO3 | 1 | 0.67 |
| HfAlO4 | 2 | 2.0 |
| HfAlO5 | 6 | 5.8 |
| HfAlO6 | 1/0 | 1/0 |

a)Electronic mail: liquan@phy.cuhk.edu.hk

 © 2007 American Institute of Physics

Downloaded 10 May 2007 to 137.189.4.1. Redistribution subject to AIP license or copyright, see http://jap.aip.org/jap/copyright.jsp

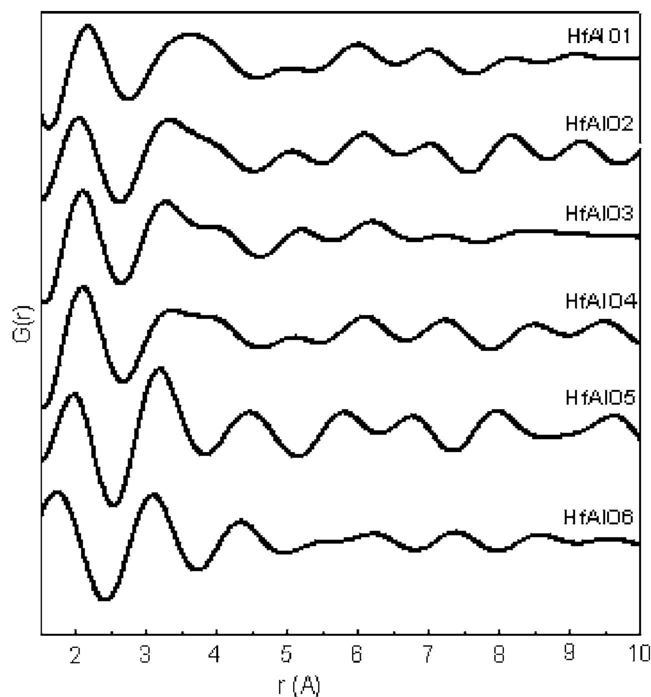


FIG. 1. Radial distribution functions of the HfAlO films.

FEG). Selected area diffraction patterns were recorded from plan-view TEM samples, the angular distribution being processed to extract the RDFs of the corresponding films.[13,14] Electron energy-loss measurements of the films were performed using the Gatan imaging filter (GIF) system attached to the same TEM, with an optimum energy resolution of 0.7 eV and a spatial resolution of ~1–5 nm.[15] The loss spectra were acquired in TEM diffraction mode with an instrumental angular resolution of about 1 mrad for the core-loss data and 0.2 mrad for the low-loss data. While the core-loss spectra were taken at essentially zero momentum transfer ($q$), the low-loss spectra were acquired at small $q$ to avoid contributions from surface plasmons and the Čerenkov effect. The energy-loss spectra were then processed using a Fourier-ratio algorithm (for the core loss) (Ref. 16) and direct deconvolution (for the low loss) (Refs. 17 and 18) to eliminate plural-scattering effects. The $f$-sum rule was employed to obtain the loss function $[\mathrm{Im}(-1/\varepsilon)]$ on an absolute scale.

## III. RESULTS AND DISCUSSION

The Al/Hf ratios of the films were deduced from XPS results (Table I). Starting from pure $HfO_2$, six films were numbered as HfAlO1 to HfAlO6 with increasing Al concentration, the last film being pure $Al_2O_3$. While all of the films were amorphous, their RDFs (Fig. 1), obtained from the selected area diffraction patterns, are different. The two main peaks in the RDF of the pure $HfO_2$ film appear at ~2.17 Å and ~3.61 Å, agreeing well with the literature-reported Hf–O and Hf–Hf bond lengths, respectively.[19] The aluminum addition, even to large percentage (up to Al/Hf=2), slightly shifts the ~2.17 Å peak to lower values (~2.10 Å) but without any obvious trend as the Al content varies. When the Al/Hf ratio is increased to 5.8, this peak is observed to shift

TABLE II. List of peak values measured from the RDFs of the HfAlO films.

| Film No. | First peak (Å) | Second peak (Å) | |
|---|---|---|---|
| HfAlO1 | 2.17 | 3.61 | |
| HfAlO2 | 2.10 | 3.27 | 4.02 |
| HfAlO3 | 2.10 | 3.27 | 4.02 |
| HfAlO4 | 2.10 | 3.27 | 4.02 |
| HfAlO5 | 1.97 | 3.19 | |
| HfAlO6 | 1.74 | 3.10 | |

further to ~1.97 Å, a value that remains larger than that observed in pure $Al_2O_3$–~1.74 Å, corresponding to the bond length of Al–O.[20] As a comparison, the effect of Al addition on the second peak at ~3.61 Å is significant. For Al/Hf ratio up to 2, the second peak splits into two components, centered at ~3.27 Å and ~4.02 Å, respectively. An abrupt change occurs when the Al/Hf ratio increases to 5.8, the RDF of which film gives a single peak at ~3.19 Å, slightly larger than the ~3.10 Å value that corresponds to the Al–Al bond length,[21] as observed in the pure $Al_2O_3$ film. A list of the peak values can be found in Table II for easy comparison.

The decrease in radial distance of the first peak upon Al addition suggests several possibilities: (1) formation of Al–O bonds, (2) reduction of the Hf–O bond length as compared to that in pure $HfO_2$, (3) increase of the Al–O bond length as compared to that of pure $Al_2O_3$, or combinations of (1)–(3). Although it is intuitive to expect that the first peak would represent an average of the Hf–O and the Al–O bond lengths, the peak position is found to be insensitive to the amount of Al introduced into the film, which suggests that the film must be understood not as a mixture of the $HfO_2$ and the $Al_2O_3$ but as a "glassy" phase of Hf, Al, and O, the first peak representing the bond length of Hf (Al)–O.

Splitting of the second peak into two peaks can also be interpreted using the Hf–Al–O glassy-phase model. The ~3.27 Å peak corresponds to the bond length of Hf (Al)–Al, with more contribution from Al–Al when the Al concentration becomes large. The ~4.02 Å peak may result from the Hf–Hf bond length modified by Al addition. Similar to the evolution of the first peak, the split-peak features are insensitive to the Al content in the film up to an Al/Hf ratio of 2. When the Al/Hf ratio is further increased to 5.8, the HfAlO film becomes similar to the pure $Al_2O_3$, giving a modified Al–Al bond length of ~3.19 Å due to Hf incorporation. Despite the glassy nature of the HfAlO film (for Al/Hf ranging from 0.25 to 5.8), we note that its structure resembles that of $HfO_2$ for Al/Hf up to 2, after which a sudden phase transition occurs, leading to a volume contraction that makes it similar to $Al_2O_3$.

Core-loss EELS corresponds to electron excitation from inner shell(s) to the empty states in the material's conduction band, and its fine structure contains abundant electronic-structure information. Such information is of particular interest in hafnium oxide, the lowest part of whose conduction band is formed by the hybridization of the Hf $d$ states and the O $p$ states.[22–24] The excitation from the O $K$ level probes the unoccupied $p$ states on the oxygen atoms. Consequently, the

Downloaded 10 May 2007 to 137.189.4.1. Redistribution subject to AIP license or copyright, see http://jap.aip.org/jap/copyright.jsp

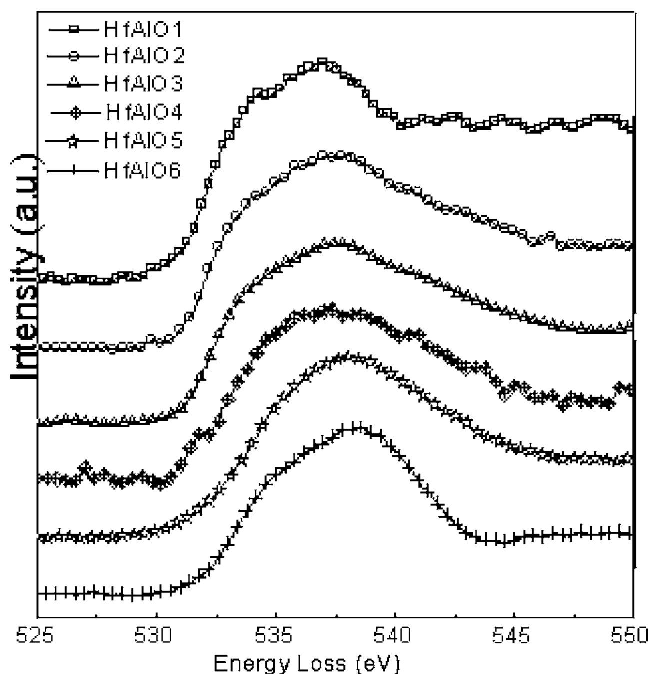


FIG. 2. Electron energy-loss spectra showing the O *K* edges of the hafnium aluminate films with different aluminum concentration.

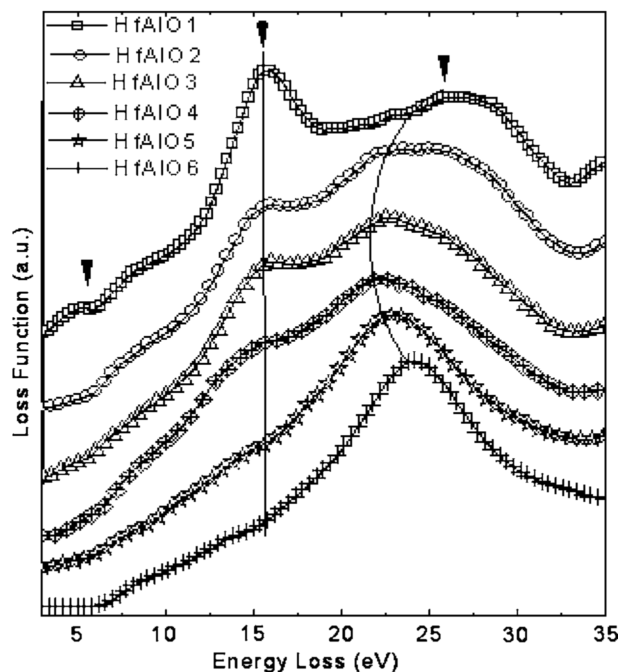


FIG. 3. Electron energy-loss spectra showing the loss functions $[\mathrm{Im}(-1/\varepsilon)]$ of the hafnium aluminate films with different aluminum concentration.

fine structures near the edge threshold reveal information on the metal atoms as a result of the strong hybridization between the O 2*p* and the Hf 5*d* orbitals. The conduction band of $Al_2O_3$, which lies higher than that of $HfO_2$, is formed by the hybridization of the Al 2*p* and the O 2*p* orbitals. This explains the larger band gap of $Al_2O_3$ compared to that of $HfO_2$ and also suggests a weak Al contribution to the O *K* near edge fine structure in the hafnium aluminate films. The core-loss spectrum of the O *K* edge taken from pure $HfO_2$ shows a major peak at ~537.5 eV and a shoulder at ~533.5 eV (Fig. 2). When Al is introduced into the film, up to Al/Hf ratio of 2, the two peaks smear out and the whole feature significantly broadens. With further increase in Al/Hf ratio to 5.8, the peak is slightly narrowed and its peak position shifts to ~538 eV, similar to that of pure $Al_2O_3$ (Ref. 25) except that the latter has an additional weak shoulder at ~535 eV.

The double-peak feature of the pure $HfO_2$ oxygen *K* edge is commonly observed in crystalline $HfO_2$, the peak separation and the depth of the minimum reflecting the specific symmetry (atomic coordination) of the Hf atom.[26] The peak separations are normally interpreted as resulting from crystal-field splitting, which requires an eightfold coordination of the Hf atom with oxygen.[27,28] Nevertheless, such a double-peak feature has also been observed in a monoclinic $HfO_2$ film, in which the cation has sevenfold coordination.[29] It is argued that a different local coordination would induce subtle differences in the peak features.[30] In the case of amorphous $HfO_2$, the observed weak splitting features (major peak at ~537.5 eV and a shoulder at ~533.5 eV) should therefore reflect the local symmetry of Hf in the absence of long-range order.[31] In several reports dealing with $HfO_2$ and $ZrO_2$, the peak separation and the depth of the minimum are also found to be sensitive to the existence of point defects,[32] which cause a filling of the gap between the two peaks. Various point defects, especially oxygen-related defects, are expected in the as-deposited $HfO_2$.[33,34] In addition, an added Al atom may itself act as a point defect (such as interstitial) or induce complex defect states by interacting with the existing defect states in the film.[35] In any case, the broad peaks observed in the range of 531–550 eV in the core-loss spectra of HfAlO films, with Al/Hf in the range of 25–2, suggest that the original local symmetry of Hf (as observed in the pure $HfO_2$) is largely destroyed by Al incorporation. At large Al concentrations (Al/Hf=5.8), the oxygen *K*-edge feature resembles that of pure $Al_2O_3$ but with larger peak width, which can be understood as a Hf doping effect. One shall expect an energy shift in the O *K* edge from $HfO_2$ to $Al_2O3$, when considering the difference in the band gap of the two. Nevertheless, such shifting is not obvious in the present data, which could be due to the small gap difference (0.8 eV) between the two materials (as commented in later sections), rough energy resolution (~1.2 eV in the core-loss EELS), and possible high tension instability during spectrum acquisitions.

Three major changes can be identified from the valence EELS spectra taken from films with different Al content. The first concerns a weak peak in the range of 3–5 eV, only discernible in pure $HfO_2$, whose intensity decreases significantly upon Al addition and totally disappears in pure $Al_2O_3$ (Fig. 3). The existence of this peak makes the determination of the material's band gap difficult. Nevertheless, estimates can be made of the band gap, and these suggest no significant effect of Al addition on the band gap (5.7 eV in pure $HfO_2$) until pure $Al_2O_3$ is reached. While the valence-band maxima of both $HfO_2$ and $Al_2O_3$ are determined by the O 2*p* states, their different band gap values (5.7 eV in $HfO_2$ versus 6.5 eV in $Al_2O_3$) mainly originate from the difference in

Downloaded 10 May 2007 to 137.189.4.1. Redistribution subject to AIP license or copyright, see http://jap.aip.org/jap/copyright.jsp

their conduction band minimum (CBM), as determined by the Hf 5$d$ states and the Al 2$p$ states in $HfO_2$ and $Al_2O_3$, respectively.[36] Therefore, the similar band gaps observed in the HfAlO films (with Al/Hf ratio in the range of 0.25–5.8) suggest that the CBM of the hafnium aluminate is mainly determined by the Hf $d$ states and/or the existence of a large number of defect states at the material's band edge. Such midgap states are also disclosed by the XPS study of the aluminate films. The better energy resolution in the XPS study enables the observation of two defect densities of states located in the center of the $HfO_2$ band gap and in the vicinity of the valence band maximum. Together with *ab initio* calculation, we found that the 3–5 eV midgap state is mainly induced by O-vacancy and interstitial-related defects. With Al taking a substitutional site in $HfO_2$, its interaction with the existing defect states leads to passivation of the charged oxygen-vacancy-induced defect bands, which explains the evolution of the midgap states, as observed in the HfAlO films.[37]

A second major change in the low-loss feature is the sharp peak at ~16 eV observed in the loss spectrum of pure $HfO_2$, which gradually decreases in intensity upon Al addition and completely disappears in films with high Al concentration (Al/Hf=5.8). Remarkably, the peak position remains unchanged for different Al contents. The third change occurs in the major broad peak in the 20–26 eV region, whose center first shifts to lower energy loss with increasing Al/Hf ratio (up to 2.2), then shifts to higher values with further increase in Al concentration until it reaches 24 eV in pure $Al_2O_3$.

The peak at 24 eV for $Al_2O_3$ is thought to be a bulk plasmon, which occurs at 26 eV for crystalline alumina and 23 eV in amorphous alumina.[38] $Al_2O_3$ has several crystalline phases, with density ranging from ~3.5 to 4.0 g/cm$^3$.[39] Taking the density value of 3.5 g/cm$^3$ as more applicable to an amorphous phase, we can estimate the plasmon energy based on a free electron model,

$$\hbar\varpi_p = \hbar\left\{\frac{N_e[(\rho/M)N_A]e^2}{m\varepsilon_0}\right\}^{1/2},$$

in which $N_e$ stands for the number of electrons per molecule, $\rho$ is the density of the material, and $M$ is the molecular weight. Depending on whether or not one counts the O 2$s$ electrons as valence electrons (resulting in 24 versus 18 valence electrons), the jellium model gives a bulk-plasmon energy of 26.1 and 22.6 eV, respectively. Band structure calculation[40,41] shows that the O 2$s$ level sits far below the valence band, and thus the 2$s$ electrons should not be counted as valence electrons. In this case, comparison with the observed value (24 eV) shows that the jellium model underestimates $E_p$ by a factor of 0.94 for alumina.

With increasing Hf content, the 24 eV peak shifts down to about 22 eV and then broadens and shifts upwards in energy, with evidence of fine structure. In addition, a prominent peak appears around ~16 eV for high Hf concentrations. In the oxides of heavy rare-earth metals ($Z$=64–71), this peak has been attributed to a bulk-plasmon resonance,[42] partly by analogy with a similar sharp peak observed at slightly lower energy (13.5–15 eV) in the rare-earth metals, where $\varepsilon_1$ crosses zero at about that energy. On a free electron model, the $HfO_2$ plasmon energy can be estimated by taking the density of 9.68 g/cm$^3$ as for the crystalline phase.[39] The most reasonable assumption (12 total valence electrons per molecule by counting eight electrons from O and four electrons from Hf) gives a plasmon energy of 21.3 eV, in which case plasmon resonance would contribute to the broad peak observed around that energy. Figure 4 shows that the measured value of the bulk plasmon energy for the whole lanthanide oxide series extended up to the hafnium oxide follows a slightly increasing law, which is similar to that deduced from the free electron model, but with absolute value typically 2–3 eV lower. Such difference becomes significant in the case of $HfO_2$, which is about 6 eV. Extending Fig. 4 to include data for three unoxidized metals ($Z$=74–76), the energy of this prominent peak increases substantially (to 25–30 eV) and so does the free electron plasmon energy. The downshift of the measured plasmon from the free electron model could be imposed by the strong oscillator strength for interband transitions at higher energies, based on the coupled oscillator theory. Nevertheless, the 6 eV downshift from that of the free electron model in the case of $HfO_2$ would require a very strong oscillator close to the plasmon loss. Interpreting the 16 eV peak as the bulk plasmon of $HfO_2$ is further supported by the dielectric functions derived from the loss function using Kramers-Kronig transformation, when the $\varepsilon_1$ plot crosses zero at ~16 eV. With such an interpretation, it remains difficult to explain the observation that the 16 eV peak remains at the same energy for all Al content, whereas a plasmon peak ought to shift as the valence-electron density changes, especially for a single-phase Hf–Al–O as suggested by the RDF results.

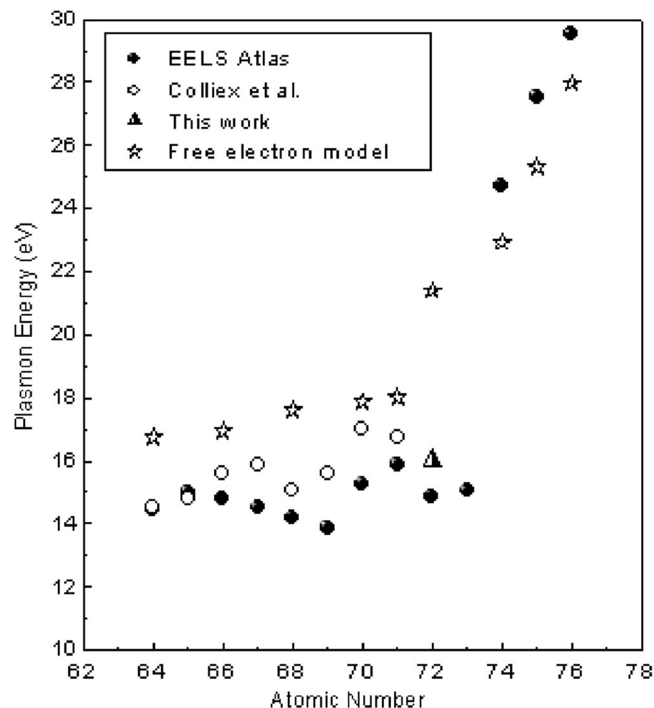


FIG. 4. Plasmon energy as a function of the atomic number, obtained from free electron model, literature works, and current study.

The shifting and broadening of the 24 eV peak (for pure

Downloaded 10 May 2007 to 137.189.4.1. Redistribution subject to AIP license or copyright, see http://jap.aip.org/jap/copyright.jsp

$Al_2O_3$) with increasing Hf content may be understood as the following. The initial downshift of the plasmon peak from pure $Al_2O_3$ to the hafnium aluminate film with Al/Hf=5.8 arises from the change in valence electron density due to the incorporation of Hf. In particular, RDF results suggest a drastic volume increase from Al/Hf=1/0 to Al/Hf=5.8/1, although the latter has a microstructure similar to that of pure $Al_2O_3$. With the Hf content continues to increase in the aluminate films, the interband transitions associated with that of $HfO_2$ become obvious, which stretch the peak features to the high energy side. On this interpretation, the broad peak and fine structure observed for pure $HfO_2$ around 26 eV arises from its interband transitions (such as those from the O 2*s* states) followed by an associated "atomic plasmon" type round maximum at ~26 eV.

## IV. CONCLUSIONS

In conclusion, we have carried out a systematic study of the evolution in microstructure and electronic structure of hafnium aluminate films, with Al concentration over the range of 0%–100%. We find that the addition of Al to $HfO_2$ leads to a glassy phase of Hf, Al, and O that resembles $HfO_2$ over a large range of Al concentration (Al/Hf ratio ranging from 0 to 2.2) and becomes similar to pure $Al_2O_3$ (in both microstructure and electronic structure) only at very high Al concentration. A degraded local symmetry of Hf (as compared to crystalline samples) is identified in the amorphous $HfO_2$. Such symmetry is effectively destroyed upon Al addition. While Al in the films has little effect on the band gap of $HfO_2$, its interaction with the native defect states leads to passivation of the midgap states in pure $HfO_2$. Although Al incorporation is expected to increase the valence-electron density of $HfO_2$, discrepancy exists in identifying the plasmon oscillation in the valence EELS spectra of the HfAlO films, although some experimental results favor interpretation of the ~16 eV peak as a bulk-plasmon oscillation.

## ACKNOWLEDGMENTS

The authors are grateful to valuable suggestions from Professor C. Colliex. The work described in this paper is supported by a grant from the Research Grants Council of the Hong Kong Special Administrative Region, China (Project No. 402105).

[1] G. D. Wilk, R. M. Wallace, and J. M. Anthony, J. Appl. Phys. **89**, 5243 (2001).
[2] R. M. Wallace and G. D. Wilk, Crit. Rev. Solid State Mater. Sci. **28**, 231 (2003).
[3] J. Robertson, Eur. Phys. J.: Appl. Phys. **28**, 265 (2004).
[4] D. A. Neumayer and E. Cartier, J. Appl. Phys. **90**, 1801 (2001).
[5] H. Y. Yu, N. Wu, M. F. Li, C. X. Zhu, and B. J. Cho, Appl. Phys. Lett. **81**, 376 (2002).
[6] W. Zhu, T. P. Ma, T. Tamagawa, J. Kim, R. Carruthers, M. Gibson, and T. Furukawa, Tech. Dig. - Int. Electron Devices Meet. **2001**, 20.4.1.
[7] Y. E. Hong, Y. S. Kim, K. Do, D. Lee, and D. H. Koa, J. Vac. Sci. Technol. A **23**, 1413 (2005).
[8] H. Y. Yu, M. F. Li, B. J. Cho, C. C. Yeo, and M. S. Joo, Appl. Phys. Lett. **81**, 376 (2002).
[9] W. J. Zhu, T. Tamagawa, M. Gibson, T. Furukawa, and T. P. Ma, IEEE Electron Device Lett. **23**, 649 (2002).
[10] S. H. Bae, C. H. Lee, R. Clark, and D. L. Kwong, IEEE Electron Device Lett. **24**, 556 (2003).
[11] M. H. Cho, D. W. Moon, S. A. Park, Y. K. Kim, and K. Jeong, Appl. Phys. Lett. **84**, 5243 (2004).
[12] Y. Q. Wang, J. H. Chen, W. J. Yoo, Y. C. Yeo, S. J. Kim, R. Gupta, and Y. L. Tan, Appl. Phys. Lett. **84**, 5407 (2004).
[13] D. J. H. Cockayne and D. R. McKenzie, Acta Crystallogr., Sect. A: Found. Crystallogr. **A44**, 870 (1988).
[14] D. J. H. Cockayne, D. R. McKenzie, W. McBride, C. Goringe, and D. McCulloch, Microsc. Microanal. **6**, 329 (2000).
[15] In principle, the spatial resolution is determined by the electron probe size, which is kept at ~1 nm during the experiments. This value is approximately the experimental spatial resolution for the core-loss spectra taken at the O *K* edge. Nevertheless, such resolution would deteriorate to ~5 nm in the low-loss spectra, as estimated by the uncertainty principle and due to the wave nature of the electrons.
[16] R. F. Egerton, *Electron Energy-Loss Spectroscopy in the Electron Microscope*, 2nd ed. (Plenum, New York, 1996).
[17] J. Daniels, C. V. Festenberg, H. Reather, and K. Zeppenfeld, *Springer Tracts in Modern Physics* (Springer, Berlin, 1970), Vol. 54.
[18] Y. Y. Wang, Ultramicroscopy **33**, 151 (1990).
[19] J. A. Speer and B. J. Cooper, Am. Mineral. **67**, 804 (1982).
[20] D. Ozkaya, W. McBride, and D. J. H. Cockayne, Interface Sci. **12**, 321 (2004).
[21] G. Gutierrez and B. Johansson, Phys. Rev. B **65**, 104202 (2002).
[22] N. I. Medvedeva, V. P. Zhukov, M. Y. Khodos, and V. A. Gubanov, Phys. Status Solidi B **160**, 517 (1990).
[23] P. K. de Boer and R. A. de Groot, J. Phys.: Condens. Matter **10**, 10241 (1998).
[24] J. Robertson, J. Vac. Sci. Technol. B **18**, 1785 (2000).
[25] I. Popava, V. Zhukov, J. T. Yates, and J. G. Chen, J. Appl. Phys. **86**, 7156 (1999).
[26] G. D. Wilk and D. A. Muller, Appl. Phys. Lett. **83**, 3984 (2003).
[27] D. W. McComb, Phys. Rev. B **54**, 7094 (1996).
[28] D. Vlachos, A. J. Craven, and D. W. McComb, J. Phys.: Condens. Matter **13**, 10799 (2001).
[29] R. H. French, S. J. Glass, F. S. Ohuchi, Y. N. Xu, and W. Y. Ching, Phys. Rev. B **49**, 5133 (1994).
[30] S. Ostanin, A. J. Craven, D. W. McComb, D. Vlachos, A. Alavi, M. W. Finnis, and A. T. Paxton, Phys. Rev. B **62**, 14728 (2000).
[31] S. Stemmer, Z. Q. Chen, W. J. Zhu, and T. P. Ma, J. Microsc. **210**, 74 (2003).
[32] B. W. Busch, O. Pluchery, Y. J. Chabal, D. A. Muller, R. L. Opila, J. R. Kwo, and E. Garfunkel, MRS Bull. **27**, 206 (2002).
[33] S. Ramanathan, D. A. Muller, G. D. Wilk, C. M. Park, and P. C. McIntyre, Appl. Phys. Lett. **79**, 3311 (2001).
[34] D. Lim, R. Haight, M. Copel, and E. Cartier, Appl. Phys. Lett. **87**, 072902 (2005).
[35] X. Guo, Phys. Status Solidi A **183**, 261 (2001).
[36] S. K. Kim, Y. Kim, and J. Hong, J. Appl. Phys. **97**, 073519 (2005).
[37] Q. Li, K. M. Koo, W. M. Lau, P. F. Lee, J. Y. Dai, Z. F. Hou, and X. G. Gong, Appl. Phys. Lett. **88**, 182903 (2006).
[38] S. D. Mo and W. Y. Ching, Phys. Rev. B **57**, 15219 (1998).
[39] I. Levin and D. Brandon, J. Am. Ceram. Soc. **81**, 1995 (1998).
[40] J. E. Jaffe, R. Pandey, and A. B. Kunz, Phys. Rev. B **43**, 14030 (1991).
[41] R. Reiche, F. Yubero, J. P. Espinos, and A. R. Gonzalez-Elipe, Surf. Sci. **457**, 199 (2000).
[42] C. Colliex, M. Gasgnier, and P. Trebbia, J. Phys. (France) **37**, 397 (1976).

**Downloaded 10 May 2007 to 137.189.4.1. Redistribution subject to AIP license or copyright, see http://jap.aip.org/jap/copyright.jsp**